Carbohydrate Polymers **21** (1993) 47–51

Scanning tunnelling microscopy of xanthan gum

A.P. Gunning, T.J. McMaster* & V.J. Morris‡

AFRC Institute of Food Research, Norwich Laboratory, Norwich Research Park, Colney, Norwich, UK, NR4 7UA

(Received 7 December 1992; revised version received 20 January 1993; accepted 1 February 1993)

Scanning tunnelling microscopy (STM) has been used to obtain images of the bacterial polysaccharide xanthan gum. The polysaccharide was deposited onto highly oriented pyrolytic graphite from a concentrated (100 mg ml^{-1}) aqueous dispersion. The viscoelastic deposit was sheared in order to induce molecular alignment and then imaged in air. STM studies revealed aggregates of stiff, aligned rod-shaped molecules.

INTRODUCTION

Despite the theoretical problems associated with explaining how scanning tunnelling microscopy (STM) can image biological molecules deposited onto conducting substrates (Welland & Taylor, 1990; Nawaz *et al.*, 1992), there is growing and convincing experimental evidence that this technique can produce high-resolution images of biopolymers (Arscott & Bloomfield, 1990; Engel, 1991; Morris & McMaster, 1991; Rabe, 1992; Schabert *et al.*, 1992). Most effort has been concentrated upon the imaging of DNA and proteins. Despite the biological importance of carbohydrates there have been very few studies of carbohydrates by STM.

Early STM studies of cyclodextrins (Miles *et al.*, 1990) used derivatised rings and the carbohydrate was imaged by default. Recently, Shigekawa *et al.* (1991) have reported studies on underivatised cyclodextrins and their complexes. Images of glycogen are claimed to show ellipsoidal structures exhibiting surface laminations attributed to short, amylose-like helical branches (Yang *et al.*, 1990). Recently, STM studies have been reported on the polysaccharides amylose (Oka & Takahashi, 1992), ι- and κ-carrageenan (Lee *et al.*, 1992), and several cellulose derivatives (Rabe *et al.*, 1990; Miles *et al.*, 1991) including preliminary studies on the cellulose related polysaccharide xanthan (Miles *et al.*, 1991). Since the present studies were completed Meyer *et al.* (1992) have reported atomic force microscopy (AFM) studies on aligned arrays of xanthan molecules deposited on mica. At present STM of biopolymers is not a routine procedure. Although there are now several papers reporting STM studies of polysaccharides none of these studies have as yet been reproduced by other researchers. There is a need to assess the effects of sample preparation and the reproducibility of STM images. Xanthan gum is one of the most widely studied polysaccharides and thus is a good candidate for examination by STM.

Xanthan is an anionic heteropolysaccharide. The chemical repeat unit structure (Fig. 1) consists of a cellulose backbone solubilised by substitution with a charged trisaccharide sidechain (βDMan (1 → 4) βDGlcA (1 → 2) αDMan (→) on alternate glucose residues (Jansson *et al.*, 1975; Melton *et al.*, 1976). In the solid state, X-ray diffraction (XRD) studies of oriented xanthan fibres have revealed that xanthan forms a five-fold helical structure with a pitch of 4·7 nm (Moorhouse *et al.*, 1977*a*, *b*; Okuyama *et al.*, 1980). Molecular modelling studies cannot at present distinguish between stereochemically allowable single or double helices, but suggest that the most likely molecular models are either a right-handed 5_1 single helix or two such helices intertwined on a common axis (Millane *et al.*, 1989; Wang, 1991). In solution conditions of high ionic strength and low temperature favour adoption of the ordered helical structure (Norton *et al.*, 1984). In the helical form xanthan is a very stiff biopolymer having a Kuhn statistical segment length in excess of 200 nm (Coviello *et al.*, 1986).

This article reports further STM studies of xanthan in its native helical structure.

*Present address: H.H. Wills Physics Laboratory, University of Bristol, Tyndall Avenue, Bristol, UK, BS8 1TL.
‡To whom correspondence should be addressed.

Carbohydrate Polymers 0144-8617/93/$06.00

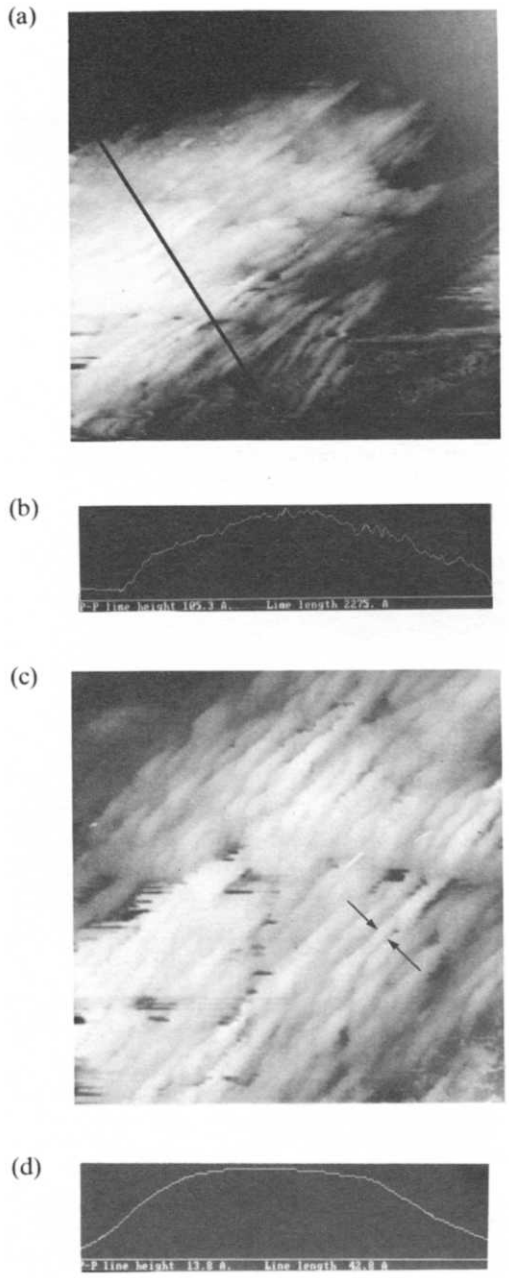

Fig. 1. Aggregates of xanthan molecules on HOPG. All images are raw data. (a) Image size 207 nm × 278 nm; tunnel current 0·1 nA; sample bias + 1 V. (b) Profile along line illustrated in Fig. 1(a) shows height and distance across the aggregate, in Å. (c) Image size 300 nm × 205 nm; tunnel current 50 pA; sample bias + 500 mV. (d) Profile of a larger rod shown between arrows in Fig. 1(c); distances are in Å. (e) Image size 121 nm × 105 nm; tunnel current 0·1 nA; sample bias +1V. (f) Profile of a typical rod in the aggregate shown between arrows in Fig. 1(e); distances are in Å.

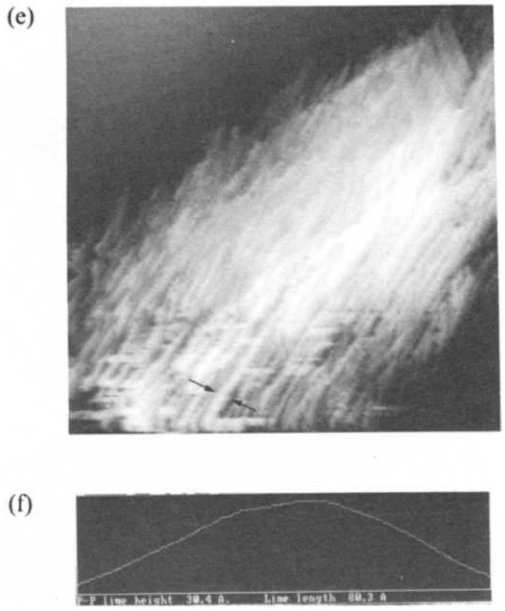

Fig. 1—*contd*

EXPERIMENTAL

Materials and methods

Xanthan gum was purchased from Kelco-AIL. The sample was a mixed salt containing sodium, potassium and calcium counterions. Residual bacterial cells were removed by dispersing the powdered sample in water (0·1% w/w) and centrifuging at 77 000 × *g* for 3 h. The pure calcium salt form was produced by passing the supernatant through a column containing H^+-ion exchange resin (DOWEX 50W-X8) and then neutralising the sample with calcium hydroxide (0·1 M solution). The neutralised dispersion was then freeze-dried.

The STM used in this study was manufactured by WA Technology (Cambridge, UK) and was operated in air, at ambient temperature and pressure, in the constant current mode with a positive sample bias. The STM tips were prepared from tungsten wire (99·9% purity, 0·5 mm diameter) by electrochemical etching in 1 M KOH. The substrate was highly oriented pyrolytic graphite (HOPG), grade ZYA, obtained from Union Carbide (USA). Fresh surfaces were produced by cleaving the graphite using adhesive tape. The quality of the tips was monitored by imaging the HOPG lattice prior to deposition of the sample, and by imaging the HOPG lattice in the vicinity of the deposited sample.

Two methods of sample deposition were used.

(i) Samples were deposited onto graphite using the drop deposition method widely used to deposit biopolymer samples for STM studies. This method was used in an attempt to exactly reproduce the previous STM studies on xanthan (Miles *et al.*, 1991). The calcium xanthan was dispersed in water at a concentration of ~ 1 $mgml^{-1}$. A 5 μl drop was deposited onto a freshly cleaved graphite surface and allowed to dry slowly. The STM was then used to scan sequentially across the deposition region.

(ii) Xanthan was deposited from a liquid crystalline

preparation. The calcium xanthan was dispersed in water at a concentration of 1 mg ml^{-1}, and then concentrated to ~ 100 mg ml^{-1} using a rotary evaporator at reduced pressure and 40°C. A small quantity of the resultant viscoelastic dispersion was deposited onto a clean glass slide and then sheared with a coverslip. When this sample was examined between crossed polarisers, areas of liquid crystalline order were observed, chiefly near the edges of the coverslip. For STM studies a similar procedure was employed. A drop of concentrated xanthan was deposited on to freshly cleaved HOPG and sheared with a coverslip. The samples were then examined using the STM. A control experiment, in which a drop of distilled water was sheared with a coverslip on freshly cleaved HOPG, was used to assess whether the shearing process damaged the HOPG surface.

RESULTS AND DISCUSSION

Examination of samples prepared by deposition from dilute solution failed to reveal any images of individual xanthan molecules or ordered arrays of xanthan molecules. It is possible that drying resulted in the formation of few large aggregates which remained undetected. An alternative explanation is that the probe interacts with the molecules effectively sweeping them outside the scan range. Such effects have been suggested by several authors (see, for example, Wilson *et al.* (1991)). More recently, Nawaz *et al.* (1992) have reported such effects for model particles deposited on HOPG.

Deposition of xanthan from concentrated dispersions resulted in the formation of large aggregates. Such large deposits were observed in samples prepared independently on four separate occasions. On each occasion several aggregated deposits could easily be found and imaged. At the edges of the deposits it was possible to image thinner aggregates, up to 15 nm in height, by STM. These images could only be obtained using slow scan speeds (typical image acquisition times were 469 s), and gap resistances, typically 10 GΩ. The gap resistance is proportional to the tip–substrate separation. At faster scan speeds and lower gap resistances the images became excessively streaky, presumably due to the probe interacting with the sample. It ws also noticed that better, more detailed images were obained if the samples were examined immediately after deposition and shearing, before they had fully dried. This is consistent with previous studies where the extent of hydration of the biomolecules being imaged by STM has been found to be important (Guckenberger *et al.*, 1989).

Figures 1(a), (c) and (e) show three examples of aggregates obtained on different occasions and observed by STM. The surface adjacent to the aggregates was flat and it was possible to image the atomic corrugation of the graphite lattice in these regions. No such large deposits were observed after exhaustive examination on the control sample indicating that these are not artefacts induced by the shearing process. The features appear to be large molecular aggregates, which by their size are probably more stable to possible tip movement effects reported elsewhere (Wilson *et al.*, 1991; Nawaz *et al.*, 1992).

The aggregates are composed of aligned bundles of rod-like particles overlaying one another. This is consistent with a concentrated liquid crystalline structure aligned by shearing. It is not easy to identify the ends of the molecules except at the extremities of the aggregates. Individual rods appear to be straight over their observable length and this is consistent with the large persistence length of xanthan helices.

A profile drawn across the whole deposit shown in Fig. 1(a) is illustrated in Fig. 1(b). This simply shows that the aggregates are not monolayers but consists of large numbers of molecules stacked on top of each other. Higher magnification scans (Figs 1(c)–(f)) reveal that the molecules are rod-like and aligned. Most of the rods are of a similar diameter and a typical profile is shown in Figs (e) and (f). If the extremities of the image are taken as the points at which the line profile reaches the baseline then the maximum width of the individual rods was found to be ~ 4·4 nm. It is unlikely that this width is a reasonable estimate of molecular diameter because any image of a cylindrical particle on a conducting substrate will be broadened and distorted by the profile of the tip (Stemmer & Engel, 1990). The width measured at half-height of the line profile will provide a better estimate of the molecular diameter. Although this is a rough and expedient approximation it does provide a criterion for determining a measured parameter which can be compared with molecular dimensions obtained by other means. Using such a criterion the molecular diameter was found to be similar for the vast majority of rods measured and to have a value of ~ 2·8 nm. Modelling of hydrodynamic data suggests a diameter for individual xanthan helices of ~ 2·2 nm (Coviello *et al.*, 1986). Thus, the majority of observed rods have diameters consistent with those expected for individual helices. There were a few rod-like objects with larger diameters (e.g. Figs 1(c) and (d)). Such objects may represent unresolved aggregates of a few molecules. Miles *et al.* (1991) using STM reported smaller diameters for xanthan (~ 1·5 nm) and Meyer *et al.* (1992) using AFM reported diameters between 1·5 and 2·0 nm. In both cases the criteria used for defining the diameter was unspecified. Without knowledge of the criteria used by others to measure molecular diameters it is not possible to comment on the values obtained in the present studies and those reported elsewhere.

Previous authors have used STM (Miles *et al.*, 1991) and AFM (Meyer *et al.*, 1992) images of xanthan to draw conclusions about the helical structure of xanthan. Miles *et al.* (1991) reported a periodicity of ~ 2·0 nm determined from line profiles measured along some of the observed molecules, and taken to be consistent with a double-helical model for xanthan. Meyer *et al.* (1992) report a measured 'helical path' of 6·2 nm, said to be consistent with XRD data on xanthan (Okuyama *et al.*, 1980). It is not clear what this 'helical path' represents or how it was measured. In the present study, although reproducible images of xanthan could be obtained, the images were not of sufficient quality to permit any analysis of the helical structure. Although the periodicities along individual regions of the rod-like molecules could be measured, the values obtained varied from region to region within a molecule and from molecule to molecule. This is illustrated in Fig. 2 which shows a Fourier transform of a region of the aggregate structure shown in Fig. 1(c). This pattern is consistent with an aligned 'liquid crystalline' array of rod-like particles. The two prominent reflections, arrowed in Fig. 2(b), are consistent with an average interparticle spacing but no long range order. There is no experimental evidence for any consistent periodic structure along the rod axes (Fig. 2(c)).

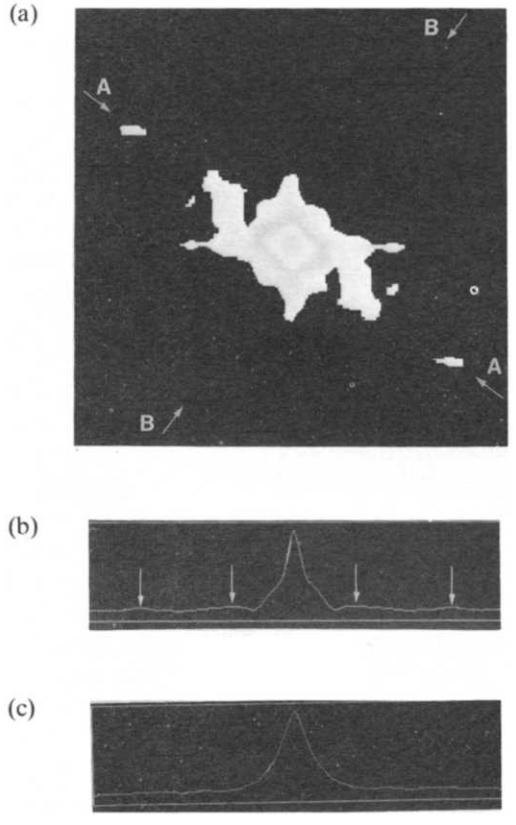

Fig. 2. (a) Fourier transform of aggregate in Fig. 2(c). (b) Profile along line AA — 2 reflections arrowed. (c) Profile along line BB — rod axis.

CONCLUSIONS

It has proved possible to obtain STM images of the bacterial polysaccharide xanthan. It was not possible to obtain images of xanthan using the conventional drop deposition method. It was found possible to obtain reproducible images by depositing xanthan onto HOPG from highly concentrated aqueous dispersions, and shearing the deposit prior to imaging. The images reveal aligned arrays of rod-like, stiff macromolecules with 'diameters' consistent with those expected for individual helices, but are of insufficient quality to permit any analysis of helical structure.

ACKNOWLEDGEMENTS

The authors wish to thank G.R. Chilvers for preparing the purified salt form of xanthan, and the referees for drawing attention to the work of Meyer *et al.* (1992).

REFERENCES

Arscott, P.G. & Bloomfield, V.A. (1990). *Trends Biotechnol.*, **8,** 151–6.

Coviello, T., Kajiwara, K., Burchard, W., Dentini, M. & Crescenzi, V. (1986). *Macromolecules,* **19,** 2826–31.

Engel, A. (1991). *Ann. Revs. Biophys. Biophysic. Chem.*, **20,** 79–108.

Guckenberger, R., Wiegräbe, W., Hillebrand, A., Hartmann, T., Wang, Z. & Baumeister, W. (1989). *Ultramicroscopy,* **31,** 327–32.

Jansson, P.E., Kenne, L. & Lindberg, B. (1975). *Carbohydr. Res.*, **45,** 275–82.

Lee, I., Atkins, E.D.T. & Miles, M.J. (1992). *Ultramicroscopy,* **42–44,** 1107–12.

Melton, L.D., Mindt, L., Rees, D.A. & Sanderson, G.R. (1976). *Carbohydr. Res.*, **46,** 245–57.

Meyer, A., Rouquet, G., Lecourtier, J. & Toulhoat, H. (1992). In *Physical Chemistry of Colloids and Interfaces in Oil Production,* eds H. Toulhoat & J. Lecourtier. Edition Technip., Paris, France, pp. 275–8.

Miles, M.J., McMaster, T.J., Carr, H.J., Tatham, A.S., Shewry, P.R., Field, J.M., Belton, P.S., Jeenes, D., Hanley, A.B., Witham, M., Cairns, P., Morris, V.J. & Lambert, N. (1990). *J. Vac. Sci. Technol.*, **A8,** 698–702.

Miles, M.J., Lee, I. & Atkins, E.D.T. (1991). *J. Vac. Sci. Technol.*, **B9,** 1189–92.

Millane, R.P., Narasaiah, T.V. & Arnott, S. (1989). In *Biomedical and Biotechnological Advances in Industrial Polysaccharides,* eds V. Crescenzi, I.C.M. Dea, S. Paoletti, S.S. Stivala & I.W. Sutherland. Gordon & Breach, New York, USA, pp. 469–78.

Moorhouse, R., Walkinshaw, M.D. & Arnott, S. (1977*a*). In *Extracellular Microbial Polysaccharides,* (ACS Symp. Ser. **45**) eds P.A. Sandford & A. Laskin. American Chemical Society, Washington DC, USA, pp. 90–102.

Moorhouse, R., Walkinshaw, M.D., Winter, W.T. & Arnott, S. (1977*b*). In *Cellulose Chemistry and Technology,* ed. J.D. Arthur. American Chemical Society, Washington DC, USA, pp. 133–52.

Morris, V.J. & McMaster, T.J. (1991). *Trends Food Sci. Technol.*, **2**, 80–84.
Nawaz, Z., Cataldi, T.R.I., Knall, J., J. Somekh, R. & Pethica, J.B. (1992). *Surface Sci.*, **265**, 139–55.
Norton, I.T., Goodall, D.M., Frangou, S.A., Morris, E.R. & Rees, D.A. (1984). *J. Mol. Biol.*, **175**, 371–94.
Oka, Y. & Takahashi, A. (1992). *Kobunshi Ronbunshi*, **49**, 389–91.
Okuyama, K., Arnott, S., Moorhouse, R., Walkinshaw, M.D., Atkins, E.D.T. & Wolf-Ullish, C.H. (1980). In *Fiber Diffraction Methods* (ACS Symp. Ser. **141**) American Chemical Society, Washington DC, USA, pp. 411–27.
Rabe, J.P. (1992). *Ultramicroscopy*, **42–44**, 41–54.
Rabe, J.P., Bucholz, S. & Ritcey, A.M. (1990). *J. Vac. Sci. Technol.*, **A8**, 679–83.
Schabert, E., Heft, A., Goldie, K., Stemmer, A., Engel, A., Meyer, E., Overney, R. & Güntherodt, H.-J. (1992). *Ultramicroscopy*, **42–44**, 1118–24.
Shigekawa, H., Morozumi, T., Komiyama, M., Yoshimura, M., Kawazu, A. & Saito, Y. (1991). *J. Vac. Sci. Technol.*, **B9**, 1189–92.
Stemmer, A. & Engel, A. (1990). *Ultramicroscopy*, **34**, 129–40.
Wang, B. (1991). MS thesis, Purdue University, West Lafayette, IN, USA.
Welland, M.E. & Taylor, M.E. (1990). In *Modern Microscopies: Techniques and Applications*, eds P.J. Duke & A.G. Michette. Plenum Press, London, New York, pp. 231–54.
Wilson, T.E., Murray, M.N., Ogletree, D.F., Bednarski, M.D., Cantor, C.R. & Salmeron, M.B. (1991). *J. Vac. Sci. Technol.*, **B9**, 1171–6.
Yang, X., Miller, M.A., Young, R., Evans, D.F. & Edstrom, R.D. (1990). *FASEB J.*, **4**, 3140–3.